Two-Scale numerical simulation of sand transport problems

Emmanuel Frenod, Ibrahima Faye, Diaraf Seck

Manuscript submitted to
AIMS' Journals
Volume **X**, Number **0X**, XX **200X**

Website: http://AIMsciences.org

pp. **X–XX**

TWO-SCALE NUMERICAL SIMULATION OF SAND TRANSPORT PROBLEMS

Ibrahima Faye

Université de Bambey,UFR S.A.T.I.C, BP 30 Bambey (Sénégal),
Ecole Doctorale de Mathématiques et Informatique.
Laboratoire de Mathématiques de la Décision et d'Analyse Numérique
(L.M.D.A.N) F.A.S.E.G)/F.S.T.

Emmanuel Frénod and Diaraf Seck

Université Européenne de Bretagne, LMBA(UMR6205)
Université de Bretagne-Sud, Centre Yves Coppens,
Campus de Tohannic, F-56017, Vannes Cedex, France
ET
Projet INRIA Calvi, Université de Strasbourg, IRMA,
7 rue René Descartes, F-67084 Strasbourg Cedex, France

Université Cheikh Anta Diop de Dakar, BP 16889 Dakar Fann,
Ecole Doctorale de Mathématiques et Informatique.
Laboratoire de Mathématiques de la Décision et d'Analyse Numérique
(L.M.D.A.N) F.A.S.E.G)/F.S.T.
ET
UMMISCO, UMI 209, IRD, France

(Communicated by the associate editor name)

[1]

Abstract. In this paper we consider the model built in [3] for short term dynamics of dunes in tidal area. We construct a Two-Scale Numerical Method based on the fact that the solution of the equation which has oscillations Two-Scale converges to the solution of a well-posed problem. This numerical method uses on Fourier series.

1. **Introduction.** This paper deals with numerical simulations of sand transport problems. Its goal is to build a Two-Scale Numerical Method to simulate dynamics of dunes in tidal area.
This paper enters a work program concerning the development of Two-Scale Numerical Methods to solve PDEs with oscillatory singular perturbations linked with physical phenomena. In Ailliot, Frénod and Monbet [2], such a method is used to manage the tide oscillation for long term drift forecast of objects in coastal ocean waters. Frénod, Mouton and Sonnendrücker [5] made simulations of the 1D Euler equation using a Two-Scale Numerical Method. In Frénod, Salvarani and Sonnendrücker [6], such a method is used to simulate a charged particle beam in a periodic focusing channel. Mouton [9, 10] developped a Two-Scale Semi Lagrangian Method for beam and plasma applications.

We consider the following model, valid for short-term dynamics of dunes, built and studied in [3]:

$$\left\{ \begin{array}{c} \dfrac{\partial z^\epsilon}{\partial t} - \dfrac{1}{\epsilon}\nabla\cdot(\mathcal{A}^\epsilon \nabla z^\epsilon) = \dfrac{1}{\epsilon}\nabla\cdot\mathcal{C}^\epsilon, \\ z^\epsilon_{|t=0} = z_0, \end{array} \right. \tag{1.1}$$

2000 *Mathematics Subject Classification.* Primary: 35K65, 35B25, 35B10 ; Secondary: 92F05, 86A60 .

Key words and phrases. Homogenization, Asymptotic Analysis, Asymptotic Expansion, Long Time Behavior, Dune and Megaripple Morphodynamics, Modeling Coastal Zone Phenomena, Numerical Simulation.

[1]This work is supported by NLAGA(Non Linear Analysis, Geometry and Application Project).

where $z^\epsilon = z^\epsilon(t,x)$ is the dimensionless seabed altitude. For a given T, $t \in (0,T)$ stands for the dimensionless time and $x \in \mathbb{T}^2$, $\mathbb{T}^2$ being the two dimensional torus $\mathbb{R}^2/\mathbb{Z}^2$, stands for the dimensionless position and $\mathcal{A}^\epsilon$, $\mathcal{C}^\epsilon$ are given by

$$\mathcal{A}^\epsilon(t,x) = \widetilde{\mathcal{A}}^\epsilon(t,x) + \epsilon\widetilde{\mathcal{A}}_1^\epsilon(t,x), \tag{1.2}$$

and

$$\mathcal{C}^\epsilon(t,x) = \widetilde{\mathcal{C}}^\epsilon(t,x) + \epsilon\widetilde{\mathcal{C}}_1^\epsilon(t,x), \tag{1.3}$$

where, for three positive constants a, b and c,

$$\widetilde{\mathcal{A}}^\epsilon(t,x) = \widetilde{\mathcal{A}}(t,\frac{t}{\epsilon},x) = a\, g_a(|\mathcal{U}(t,\frac{t}{\epsilon},x)|), \tag{1.4}$$

$$\widetilde{\mathcal{C}}^\epsilon(t,x) = \widetilde{\mathcal{C}}(t,\frac{t}{\epsilon},x) = c\, g_c(|\mathcal{U}(t,\frac{t}{\epsilon},x)|)\,\frac{\mathcal{U}(t,\frac{t}{\epsilon},x)}{|\mathcal{U}(t,\frac{t}{\epsilon},x)|}, \tag{1.5}$$

and

$$\widetilde{\mathcal{A}}_1^\epsilon(t,x) = \widetilde{\mathcal{A}}_1(t,\frac{t}{\epsilon},x),\ \widetilde{\mathcal{C}}_1^\epsilon(t,x) = \widetilde{\mathcal{C}}_1(t,\frac{t}{\epsilon},x), \tag{1.6}$$

with

$$\widetilde{\mathcal{A}}_1(t,\theta,x) = -ab\mathcal{M}(t,\theta,x)\, g_a(|\mathcal{U}(t,\theta,x)|) \text{ and } \widetilde{\mathcal{C}}_1(t,\theta,x) = -cb\mathcal{M}(t,\theta,x)\, g_c(|\mathcal{U}(t,\theta,x)|)\,\frac{\mathcal{U}(t,\theta,x)}{|\mathcal{U}(t,\theta,x)|}. \tag{1.7}$$

$\mathcal{U}$ and $\mathcal{M}$ are the dimensionless water velocity and height.
The small parameter ϵ involved in the model is the ratio between the main tide period $\frac{1}{\bar{\omega}} = 13$ hours and an observation time which is about three months i.e. $\epsilon = \frac{1}{t\bar{\omega}} = \frac{1}{200}$.
The following hypotheses on g_a, g_c, $\mathcal{U}$ and $\mathcal{M}$ given in (1.8) and (1.9) are technical assumptions and are needed to prove Theorem 1.1. Functions g_a and g_c are regular functions on $\mathbb{R}^+$ and satisfy

$$\begin{cases} g_a \geq g_c \geq 0,\ g_c(0) = g_c'(0) = 0, \\ \exists\, d \geq 0, \sup_{u\in\mathbb{R}^+}|g_a(u)| + \sup_{u\in\mathbb{R}^+}|g_a'(u)| \leq d, \\ \sup_{u\in\mathbb{R}^+}|g_c(u)| + \sup_{u\in\mathbb{R}^+}|g_c'(u)| \leq d, \\ \exists\, U_{thr} \geq 0,\ \exists\, G_{thr} > 0,\ \text{such that } u \geq U_{thr} \Longrightarrow g_a(u) \geq G_{thr}. \end{cases} \tag{1.8}$$

Functions $\mathcal{U}$ and $\mathcal{M}$ are regular and satisfy:

$$\begin{cases} \theta \longmapsto (\mathcal{U},\mathcal{M}) \text{ is periodic of period } 1, \\ |\mathcal{U}|,\ |\frac{\partial\mathcal{U}}{\partial t}|,\ |\frac{\partial\mathcal{U}}{\partial\theta}|,\ |\nabla\mathcal{U}|, \\ |\mathcal{M}|,\ |\frac{\partial\mathcal{M}}{\partial t}|,\ |\frac{\partial\mathcal{M}}{\partial\theta}|,\ |\nabla\mathcal{M}| \text{ are bounded by } d, \\ \forall\,(t,\theta,x) \in \mathbb{R}^+\times\mathbb{R}\times\mathbb{T}^2,\ |\mathcal{U}(t,\theta,x)| \leq U_{thr} \Longrightarrow \\ \Big(\frac{\partial\mathcal{U}}{\partial t}(t,\theta,x) = 0,\ \nabla\mathcal{U}(t,\theta,x) = 0, \\ \frac{\partial\mathcal{M}}{\partial t}(t,\theta,x) = 0,\ \text{ and } \nabla\mathcal{M}(t,\theta,x) = 0\Big), \\ \exists\,\theta_\alpha < \theta_\omega \in [0,1] \text{ such that } \forall\,\theta \in [\theta_\alpha,\theta_\omega] \Longrightarrow |\mathcal{U}(t,\theta,x)| \geq U_{thr}. \end{cases} \tag{1.9}$$

To develop the Two-Scale Numerical Method, we use that in [3] we proved that under assumptions (1.8) and (1.9) the solution z^ϵ of (1.1) exists, is unique and moreover asymptotically behaves, as $\epsilon \to 0$, the way given by the following theorem.

Theorem 1.1. *Under assumptions (1.8) and (1.9), for any T, not depending on ϵ, the sequence (z^ϵ) of solutions to (1.1), with coefficients given by (1.2) coupled with (1.4) and (1.3), (1.5) and (1.6), Two-Scale converges to the profile $Z \in L^\infty([0,T], L^\infty_\#(\mathbb{R}, L^2(\mathbb{T}^2)))$ solution to*

$$\frac{\partial Z}{\partial\theta} - \nabla\cdot(\widetilde{\mathcal{A}}\nabla Z) = \nabla\cdot\widetilde{\mathcal{C}}, \tag{1.10}$$

where $\widetilde{\mathcal{A}}$ and $\widetilde{\mathcal{C}}$ are given by

$$\widetilde{\mathcal{A}}(t,\theta,x) = a\, g_a(|\mathcal{U}(t,\theta,x)|) \text{ and } \widetilde{\mathcal{C}}(t,\theta,x) = c\, g_c(|\mathcal{U}(t,\theta,x)|)\,\frac{\mathcal{U}(t,\theta,x)}{|\mathcal{U}(t,\theta,x)|}. \tag{1.11}$$

Futhermore, if the supplementary assumption

$$U_{thr} = 0, \tag{1.12}$$

is done, we have

$$\widetilde{\mathcal{A}}(t,\theta,x) \geq \widetilde{G}_{thr} \text{ for any } t,\theta,x \in [0,T]\times\mathbb{R}\times\mathbb{T}^2, \tag{1.13}$$

and, defining $Z^\epsilon = Z^\epsilon(t,x) = Z(t,\frac{t}{\epsilon},x)$*, the following estimate holds for* $z^\epsilon - Z^\epsilon$

$$\Big\|\frac{z^\epsilon - Z^\epsilon}{\epsilon}\Big\|_{L^\infty([0,T),L^2(\mathbb{T}^2))} \leq \alpha, \tag{1.14}$$

where α *is a constant not depending on* ϵ*.*

Because of assumptions (1.8) and (1.9),

$$\widetilde{\mathcal{A}},\ \widetilde{\mathcal{C}},\ \widetilde{\mathcal{A}}_1,\ \widetilde{\mathcal{C}}_1,\ \widetilde{\mathcal{A}}^\epsilon,\ \widetilde{\mathcal{A}}_1^\epsilon,\ \widetilde{\mathcal{C}}^\epsilon, \text{ and } \widetilde{\mathcal{C}}_1^\epsilon \text{ are regular and bounded.} \tag{1.15}$$

2. **Two-Scale Numerical Method Building.** In this section, we develop the Two-Scale Numerical Method in order to approach the solution z^ϵ of (1.1). The idea is to get a good approximation of $z^\epsilon(t,x)$ seeing Theorem 1.1 content as $z^\epsilon(t,x) \sim Z(t,\frac{t}{\epsilon},x)$.
The strategy is to consider a Fourier expansion of Z solution to (1.10). In this equation, t is only a parameter.
The Fourier expansion of Z is given as follows:

$$Z(t,\theta,x) = \sum_{l,m,n} Z_{l,m,n}(t)\ e^{2i\pi(l\theta+mx_1+nx_2)}, \tag{2.1}$$

where $Z_{l,m,n}(t)$, $l = 0,1,2,\ldots$, $m = 0,1,2,\ldots$, $n = 0,1,2,\ldots$, are the unknown complex coefficients of the Fourier expansion of Z. Using (2.1), the Fourier expansion of $\frac{\partial Z}{\partial\theta}$ is given by

$$\frac{\partial Z}{\partial\theta}(t,\theta,x) = \sum_{l,m,n} 2i\pi\, l\, Z_{l,m,n}(t)\ e^{2i\pi(l\theta+mx_1+nx_2)}. \tag{2.2}$$

To obtain the system satisfied by the Fourier expansion (2.1) of Z, it is necessary to compute the Fourier expansions of $\nabla\cdot(\widetilde{\mathcal{A}}\nabla Z)$ and $\nabla\cdot\widetilde{\mathcal{C}}$. As $\nabla\cdot(\widetilde{\mathcal{A}}\nabla Z) = \nabla\widetilde{\mathcal{A}}\cdot\nabla Z + \widetilde{\mathcal{A}}\cdot\Delta Z$, let

$$\sum_{l,m,n} \widetilde{\mathcal{A}}_{l,m,n}(t)\, e^{2i\pi(l\theta+mx_1+nx_2)}, \tag{2.3}$$

and

$$\sum_{l,m,n} \widetilde{\mathcal{A}}^{grad}_{l,m,n}(t)\, e^{2i\pi(l\theta+mx_1+nx_2)}, \tag{2.4}$$

be respectively the Fourier expansions of $\widetilde{\mathcal{A}}$ and $\nabla\widetilde{\mathcal{A}}$, where $\widetilde{\mathcal{A}}^{grad}_{l,m,n}(t) = 2i\pi\widetilde{\mathcal{A}}_{l,m,n}\begin{pmatrix} m \\ n \end{pmatrix}$ and then the Fourier expansions of ∇Z and ΔZ are respectively given by

$$\sum_{l,m,n} 2i\pi\begin{pmatrix} m \\ n \end{pmatrix} Z_{l,m,n}(t)\, e^{2i\pi(l\theta+mx_1+nx_2)}, \tag{2.5}$$

and

$$-\sum_{l,m,n} 4\pi^2(m^2+n^2) Z_{l,m,n}(t)\, e^{2i\pi(l\theta+mx_1+nx_2)}. \tag{2.6}$$

In the same way the Fourier expansion of $\nabla\cdot\widetilde{\mathcal{C}}$ is given by

$$\sum_{l,m,n} \widetilde{\mathcal{C}}_{l,m,n} e^{2i\pi(l\theta+mx_1+nx_2)}. \tag{2.7}$$

Using (2.1), (2.2), (2.3), (2.4), (2.5), (2.6) and (2.7), equation (1.10) becomes

$$\begin{aligned}
&\sum_{l,m,n} 2i\pi\, l\, Z_{l,m,n}(t)\ e^{2i\pi(l\theta+mx_1+nx_2)} \\
&-\Big(\sum_{l,m,n} \widetilde{\mathcal{A}}^{grad}_{l,m,n}(t)\, e^{2i\pi(l\theta+mx_1+nx_2)}\Big)\cdot\Big(\sum_{l,m,n} 2i\pi\begin{pmatrix} m \\ n \end{pmatrix} Z_{l,m,n}(t)\, e^{2i\pi(l\theta+mx_1+nx_2)}\Big) \\
&+\Big(\sum_{l,m,n} \widetilde{\mathcal{A}}_{l,m,n}(t)\, e^{2i\pi(l\theta+mx_1+nx_2)}\Big)\Big(\sum_{l,m,n} 4\pi^2(m^2+n^2) Z_{l,m,n}(t)\, e^{2i\pi(l\theta+mx_1+nx_2)}\Big) = \\
&\sum_{l,m,n} \widetilde{\mathcal{C}}_{l,m,n}(t)\, e^{2i\pi(l\theta+mx_1+nx_2)},
\end{aligned} \tag{2.8}$$

which gives after identification, the following algebraic system for $(Z_{l,m,n})$:

$$2i\pi\, l\, Z_{l,m,n}(t) - \sum_{i,j,k} 2i\pi \widetilde{\mathcal{A}}^{grad}_{i,j,k}(t) \cdot \begin{pmatrix} m-j \\ n-k \end{pmatrix} Z_{l-i,m-j,n-k}(t)$$
$$+4\pi^2 \sum_{i,j,k} \widetilde{\mathcal{A}}_{i,j,k}(t)((m-j)^2+(n-k)^2) Z_{l-i,m-j,n-k}(t) = \widetilde{\mathcal{C}}_{l,m,n}(t). \tag{2.9}$$

In formula (2.1), the integers m, n and l vary from $-\infty$ to $+\infty$. But in practice, we will consider the truncated Fourier series of order $P \in \mathbb{N}$ defined by

$$Z_P(t,\theta,x) = \sum_{0\le l\le P, 0\le m\le P, 0\le n\le P} Z_{l,m,n}(t)\; e^{2i\pi(l\theta+mx_1+nx_2)}. \tag{2.10}$$

Using (2.10), formula (2.9) becomes:

$$2i\pi\, l\, Z_{l,m,n}(t) - \sum_{0\le i\le P,\, 1\le j\le P,\, 0\le k\le P} 2i\pi \widetilde{\mathcal{A}}^{grad}_{i,j,k}(t) \cdot \begin{pmatrix} m-j \\ n-k \end{pmatrix} Z_{l-i,m-j,n-k}(t)$$
$$+4\pi^2 \sum_{0\le i\le P,\, 0\le j\le P,\, 0\le k\le P} \widetilde{\mathcal{A}}_{i,j,k}(t)((m-j)^2+(n-k)^2) Z_{l-i,m-j,n-k}(t) = \widetilde{\mathcal{C}}_{l,m,n}(t). \tag{2.11}$$

3. **Convergence result.**

Proof. of Theorem 1.1. For self-containedness, we recall the proof of Theorem 1.1. Firstly, we obtain an estimate leading to that z^ϵ is bounded in $L^\infty((0,T);L^2(\mathbb{T}^2))$. Secondly, defining test function $\psi^\epsilon(t,x) = \psi(t,\frac{t}{\epsilon},x)$ for any $\psi(t,\theta,x)$, regular with a compact support over $[0,T)\times\mathbb{T}^2$ and 1-periodic in θ, multiplying (1.1) by ψ^ϵ and integrating over $[0,T)\times\mathbb{T}^2$ gives

$$\int_{\mathbb{T}^2}\int_0^T \frac{\partial z^\epsilon}{\partial t}\psi^\epsilon dtdx - \frac{1}{\epsilon}\int_{\mathbb{T}^2}\int_0^T \nabla\cdot(\mathcal{A}^\epsilon\nabla z^\epsilon)\psi^\epsilon dtdx = \frac{1}{\epsilon}\int_{\mathbb{T}^2}\int_0^T \nabla\cdot\mathcal{C}^\epsilon\psi^\epsilon dtdx. \tag{3.1}$$

Then integrating by parts in the first integral over $[0,T)$ and using the Green formula in $\mathbb{T}^2$ in the second integral we have

$$-\int_{\mathbb{T}^2} z_0(x)\psi(0,0,x)dx - \int_{\mathbb{T}^2}\int_0^T \frac{\partial\psi^\epsilon}{\partial t} z^\epsilon dtdx$$
$$+\frac{1}{\epsilon}\int_{\mathbb{T}^2}\int_0^T \mathcal{A}^\epsilon\nabla z^\epsilon\nabla\psi^\epsilon dtdx = \frac{1}{\epsilon}\int_{\mathbb{T}^2}\int_0^T \nabla\cdot\mathcal{C}^\epsilon\psi^\epsilon dtdx. \tag{3.2}$$

Again using the Green formula in the third integral we obtain

$$-\int_{\mathbb{T}^2} z_0(x)\psi(0,0,x)\,dx - \int_{\mathbb{T}^2}\int_0^T \frac{\partial\psi^\epsilon}{\partial t} z^\epsilon dtdx$$
$$-\frac{1}{\epsilon}\int_{\mathbb{T}^2}\int_0^T z^\epsilon\,\nabla\cdot(\mathcal{A}^\epsilon\nabla\psi^\epsilon)\,dtdx = \frac{1}{\epsilon}\int_{\mathbb{T}^2}\int_0^T \nabla\cdot\mathcal{C}^\epsilon\psi^\epsilon dtdx. \tag{3.3}$$

But

$$\frac{\partial\psi^\epsilon}{\partial t} = \left(\frac{\partial\psi}{\partial t}\right)^\epsilon + \frac{1}{\epsilon}\left(\frac{\partial\psi}{\partial\theta}\right)^\epsilon, \tag{3.4}$$

where

$$\left(\frac{\partial\psi}{\partial t}\right)^\epsilon(t,x) = \frac{\partial\psi}{\partial t}(t,\frac{t}{\epsilon},x) \;\text{ and }\; \left(\frac{\partial\psi}{\partial\theta}\right)^\epsilon(t,x) = \frac{\partial\psi}{\partial\theta}(t,\frac{t}{\epsilon},x), \tag{3.5}$$

then we have

$$\int_{\mathbb{T}^2}\int_0^T z^\epsilon\left(\left(\frac{\partial\psi}{\partial t}\right)^\epsilon + \frac{1}{\epsilon}\left(\frac{\partial\psi}{\partial\theta}\right)^\epsilon + \frac{1}{\epsilon}\nabla\cdot(\mathcal{A}^\epsilon\nabla\psi^\epsilon)\right)dxdt$$
$$+\frac{1}{\epsilon}\int_{\mathbb{T}^2}\int_0^T \nabla\cdot\mathcal{C}^\epsilon\psi^\epsilon dtdx = -\int_{\mathbb{T}^2} z_0(x)\psi(0,0,x)\,dx. \tag{3.6}$$

Using the Two-Scale convergence due to Nguetseng [11] and Allaire [1] (see also Frénod Raviart and Sonnendrücker [7]), since z^ϵ is bounded in $L^\infty([0,T),L^2(\mathbb{T}^2))$, there exists a profile $Z(t,\theta,x)$, periodic of period 1 with respect to θ, such that for all $\psi(t,\theta,x)$, regular with a compact support with respect to (t,x) and 1-periodic with respect to θ, we have

$$\int_{\mathbb{T}^2}\int_0^T z^\epsilon\psi^\epsilon dtdx \longrightarrow \int_{\mathbb{T}^2}\int_0^T\int_0^1 Z\psi\, d\theta dtdx, \text{ as } \epsilon \text{ tends to zero,} \tag{3.7}$$

for a subsequence extracted from (z^ϵ).
Multiplying (3.6) by ϵ, passing to the limit as $\epsilon \to 0$ and using (3.7) we have

$$\int_{\mathbb{T}^2}\int_0^T\int_0^1 Z\frac{\partial\psi}{\partial\theta}\,d\theta dtdx + \lim_{\epsilon\to 0}\int_{\mathbb{T}^2}\int_0^T z^\epsilon\nabla\cdot(\mathcal{A}^\epsilon\nabla\psi^\epsilon)\,dtdx = \lim_{\epsilon\to 0}\int_{\mathbb{T}^2}\int_0^T \mathcal{C}^\epsilon\cdot\nabla\psi^\epsilon dtdx, \tag{3.8}$$

for an extracted subsequence. As $\mathcal{A}^\epsilon$ and $\mathcal{C}^\epsilon$ are bounded and ψ^ϵ is a regular function, $\mathcal{A}^\epsilon\nabla\psi^\epsilon$ and $\nabla\psi^\epsilon$ can be considered as test functions. Using (3.7) we have

$$\int_{\mathbb{T}^2}\int_0^T z^\epsilon\,\nabla\cdot(\mathcal{A}^\epsilon\nabla\psi^\epsilon)dtdx \longrightarrow \int_{\mathbb{T}^2}\int_0^T\int_0^1 Z\nabla\cdot(\widetilde{\mathcal{A}}\nabla\psi)\,d\theta dtdx, \tag{3.9}$$

and

$$\int_{\mathbb{T}^2}\int_0^T \mathcal{C}^\epsilon\cdot\nabla\psi^\epsilon dtdx \text{ Two-Scale converges to } \int_{\mathbb{T}^2}\int_0^T\int_0^1 \widetilde{\mathcal{C}}\cdot\nabla\psi\,d\theta dtdx. \tag{3.10}$$

Passing to the limit as $\epsilon \to 0$ we obtain from (3.8) a weak formulation of the equation (1.10) satisfied by Z.
Using (1.2) and (1.3) equation (1.1) becomes

$$\frac{\partial z^\epsilon}{\partial t} - \frac{1}{\epsilon}\nabla\cdot(\widetilde{\mathcal{A}}^\epsilon\nabla z^\epsilon) = \frac{1}{\epsilon}\nabla\cdot\widetilde{\mathcal{C}}^\epsilon + \nabla\cdot(\widetilde{\mathcal{A}}_1^\epsilon\nabla z^\epsilon) + \nabla\cdot\widetilde{\mathcal{C}}_1^\epsilon. \tag{3.11}$$

For Z^ϵ, we have

$$\frac{\partial Z^\epsilon}{\partial t} = \left(\frac{\partial Z}{\partial t}\right)^\epsilon + \frac{1}{\epsilon}\left(\frac{\partial Z}{\partial\theta}\right)^\epsilon, \tag{3.12}$$

where

$$\left(\frac{\partial Z}{\partial t}\right)^\epsilon(t,x) = \frac{\partial Z}{\partial t}(t,\frac{t}{\epsilon},x) \text{ and } \left(\frac{\partial Z}{\partial\theta}\right)^\epsilon(t,x) = \frac{\partial Z}{\partial\theta}(t,\frac{t}{\epsilon},x). \tag{3.13}$$

Using (1.10), Z^ϵ is solution to

$$\frac{\partial Z^\epsilon}{\partial t} - \frac{1}{\epsilon}\nabla\cdot\left(\widetilde{\mathcal{A}}^\epsilon\nabla Z^\epsilon\right) = \frac{1}{\epsilon}\nabla\cdot\widetilde{\mathcal{C}}^\epsilon + \left(\frac{\partial Z}{\partial t}\right)^\epsilon. \tag{3.14}$$

Formulas (3.11) and (3.14) give

$$\frac{\partial(z^\epsilon - Z^\epsilon)}{\partial t} - \frac{1}{\epsilon}\nabla\cdot\left(\widetilde{\mathcal{A}}^\epsilon\nabla(z^\epsilon - Z^\epsilon)\right) = \nabla\cdot\widetilde{\mathcal{C}}_1^\epsilon + \left(\frac{\partial Z}{\partial t}\right)^\epsilon + \nabla\cdot(\widetilde{\mathcal{A}}_1^\epsilon\nabla z^\epsilon). \tag{3.15}$$

Multiplying equation (3.15) by $\frac{1}{\epsilon}$ and using the fact that $z^\epsilon = z^\epsilon - Z^\epsilon + Z^\epsilon$ in the right hand side of equation (3.15), $\frac{z^\epsilon - Z^\epsilon}{\epsilon}$ is solution to:

$$\frac{\partial\Big(\frac{z^\epsilon - Z^\epsilon}{\epsilon}\Big)}{\partial t} - \frac{1}{\epsilon}\nabla\cdot\Big((\widetilde{\mathcal{A}}^\epsilon + \epsilon\widetilde{\mathcal{A}}_1^\epsilon)\nabla(\frac{z^\epsilon - Z^\epsilon}{\epsilon})\Big) = \frac{1}{\epsilon}\Big(\nabla\cdot\widetilde{\mathcal{C}}_1^\epsilon + (\frac{\partial Z}{\partial t})^\epsilon + \nabla\cdot(\widetilde{\mathcal{A}}_1^\epsilon\nabla Z^\epsilon)\Big). \tag{3.16}$$

Our aim here is to prove that $\frac{z^\epsilon - Z^\epsilon}{\epsilon}$ is bounded by a constant α not depending on ϵ. For this let us use that $\widetilde{\mathcal{A}}^\epsilon$, $\widetilde{\mathcal{A}}_1^\epsilon$, $\widetilde{\mathcal{C}}^\epsilon$ and $\widetilde{\mathcal{C}}_1^\epsilon$ are regular and bounded coefficients (see (1.15)) and that $\widetilde{\mathcal{A}}^\epsilon \geq G_{thr}$ (see (1.13)). Hence, $\nabla\cdot\widetilde{\mathcal{C}}_1^\epsilon$ is bounded, $\nabla\cdot(\widetilde{\mathcal{A}}_1^\epsilon\nabla Z^\epsilon)$ is also bounded. Since Z^ϵ is solution to (3.14), $\frac{\partial Z}{\partial t}$ satisfies the following equation

$$\frac{\partial\left(\frac{\partial Z}{\partial t}\right)}{\partial\theta} - \nabla\cdot\left(\widetilde{\mathcal{A}}\nabla\frac{\partial Z}{\partial t}\right) = \frac{\partial\nabla\cdot\widetilde{\mathcal{C}}}{\partial t} + \nabla\cdot\left(\frac{\partial\widetilde{\mathcal{A}}}{\partial t}\nabla Z\right). \tag{3.17}$$

Equation (3.17) is linear with regular and bounded coefficients. Using a result of Ladyzenskaja, Solonnikov and Ural'Ceva [8], $\frac{\partial Z}{\partial t}$ is regular and bounded and so the coefficients of equations (3.16) are regular and bounded. Then, using the same arguments as in the proof of Theorem 1.1 in [3] we obtain that $\left(\frac{z^\epsilon - Z^\epsilon}{\epsilon}\right)$ is bounded.
To determine the value of the constant α, we proceed in the same way as in the proof of Theorem 3.16 of [3]. Since the coefficients $\Big(\widetilde{\mathcal{A}}^\epsilon,\ \widetilde{\mathcal{A}}_1^\epsilon,\ \widetilde{\mathcal{C}}^\epsilon$ and $\widetilde{\mathcal{C}}_1^\epsilon,\ \nabla\cdot\widetilde{\mathcal{C}}_1^\epsilon,\ \nabla\cdot(\widetilde{\mathcal{A}}_1^\epsilon\nabla Z^\epsilon)$, and $\frac{\partial Z}{\partial t}\Big)$ are bounded by constants, let β denotes the maximum between all these constants. Then we use the same argument as in the proof of Theorems 1.1 and 3.16 and we get:

$$\Big\|\frac{z^\epsilon - Z^\epsilon}{\epsilon}\Big\|_{L^\infty([0,T),L^2(\mathbb{T}^2))} \leq \|z_0(\cdot) - Z(0,0,\cdot)\|_2\sqrt{\frac{\beta+\beta^3}{\sqrt{\widetilde{G}_{thr}}} + 2\beta\,T}. \tag{3.18}$$

□

Theorem 3.1. *Let ϵ be a positive real, z^ϵ be the solution to (1.1), Z_P be the truncated Fourier series (defined by (2.10)) of Z solution to (1.10) and Z_P^ϵ defined by $Z_P^\epsilon(t,x) = Z_P(t, \frac{t}{\epsilon}, x)$. Then, under assumptions (1.8), (1.9) and (1.12), $z^\epsilon - Z_P^\epsilon$ satisfies the following estimate:*

$$\|z^\epsilon - Z_P^\epsilon\|_{L^\infty([0,T),L^2(\mathbb{T}^2))} \leq \epsilon \|z_0(\cdot) - Z(0,0,\cdot)\|_2 \sqrt{\frac{\beta+\beta^3}{\sqrt{\widetilde{G}_{thr}}} + 2\beta}\, T + f(P), \tag{3.19}$$

where f is a non-negative function of P not depending on ϵ and satisfying $\lim_{P\to+\infty} f(P) = 0$.

Proof. We can write:

$$\begin{aligned}\|z^\epsilon - Z_P^\epsilon\|_{L^\infty([0,T),L^2(\mathbb{T}^2))} &= \|z^\epsilon - Z^\epsilon + Z^\epsilon - Z_p^\epsilon\|_{L^\infty([0,T),L^2(\mathbb{T}^2))} \\ &\leq \|z^\epsilon - Z^\epsilon\|_{L^\infty([0,T),L^2(\mathbb{T}^2))} + \|Z^\epsilon - Z_p^\epsilon\|_{L^\infty([0,T),L^2(\mathbb{T}^2))}.\end{aligned} \tag{3.20}$$

Using (3.18), the first term in the right hand side of (3.20) is bounded by

$$\|z^\epsilon - Z^\epsilon\|_{L^\infty([0,T),L^2(\mathbb{T}^2))} \leq \epsilon \|z_0(\cdot) - Z(0,0,\cdot)\|_2 \sqrt{\frac{\beta+\beta^3}{\sqrt{\widetilde{G}_{thr}}} + 2\beta T}. \tag{3.21}$$

For the second term of (3.20), using classical results of Fourier series theory, since $Z - Z_P$ is nothing but the rest of the Fourier series of order P of Z and since Z is regular (because it is the solution of (1.10) which has regular coefficients), the non-negative function f satisfying $\lim_{P\to+\infty} f(P) = 0$ such that

$$\|Z - Z_p\|_{L^\infty([0,T],L^\infty_\#(\mathbb{R},L^2(\mathbb{T}^2)))} \leq f(P), \tag{3.22}$$

exists. From this last inequality,

$$\|Z^\epsilon - Z_p^\epsilon\|_{L^\infty([0,T),L^2(\mathbb{T}^2))} \leq f(P), \tag{3.23}$$

follows and coupling this with (3.21) and (3.20) gives inequality (3.19). □

4. Numerical illustration of Theorem 3.1.

4.1. Reference solution.

Having Fourier coefficients of Z on hand, we will do the same for function $z^\epsilon(t,x)$ solution to (1.1) in order to compare it to the profile Z for a given ϵ, in a fixed time. The Fourier expansion of z^ϵ is given by

$$z^\epsilon(t,x_1,x_2) = \sum_{m,n} z_{m,n}(t)\; e^{2\pi i(mx_1+nx_2)}, \tag{4.1}$$

where $m = 0,1,2,\dots$ and $n = 0,1,2,\dots$, then the Fourier expansion of $\frac{\partial z^\epsilon}{\partial t}$ is

$$\frac{\partial z^\epsilon}{\partial t} = \sum_{m,n} \dot{z}_{m,n}(t)\; e^{2\pi i(mx_1+nx_2)}. \tag{4.2}$$

Using the same idea as in the Fourier expansion of Z, we obtain the following infinite system of Ordinary Differential Equations

$$\begin{aligned}&\frac{\partial z_{m,n}}{\partial t}(t) - \frac{1}{\epsilon}\sum_{i,j} 2i\pi \mathcal{A}_{i,j}^{grad}(t)\cdot\begin{pmatrix} m-i \\ n-j\end{pmatrix} z_{m-i,n-j}(t) \\ &+\frac{1}{\epsilon}4\pi^2\sum_{i,j}\mathcal{A}_{i,j}(t)((m-i)^2+(n-j)^2)z_{m-i,n-j}(t) = \frac{1}{\epsilon}\mathcal{C}_{m,n}(t),\end{aligned} \tag{4.3}$$

where $\mathcal{A}_{i,j}^{grad}(t)$, $\mathcal{A}_{i,j}(t)$ and $\mathcal{C}_{m,n}(t)$ are respectively the Fourier coefficients of $\nabla\mathcal{A}^\epsilon$, $\mathcal{A}^\epsilon$ and $\nabla\cdot\mathcal{C}^\epsilon$.
In the same way, the truncated Fourier series of order $P \in \mathbb{N}$ of z^ϵ is given by

$$z_P^\epsilon(t,x_1,x_2) = \sum_{m,n=0}^{P} z_{m,n}(t)\; e^{2\pi i(mx_1+nx_2)}, \tag{4.4}$$

which gives from (4.3) the following system Ordinary Differential Equations

$$\begin{aligned}&\frac{\partial z_{m,n}}{\partial t}(t) - \frac{1}{\epsilon}\sum_{i,j=0}^{P} 2i\pi \mathcal{A}_{i,j}^{grad}(t)\cdot\begin{pmatrix} m-i \\ n-j\end{pmatrix} z_{m-i,n-j}(t) \\ &+\frac{1}{\epsilon}4\pi^2\sum_{i,j=0}^{P}\mathcal{A}_{i,j}(t)((m-i)^2+(n-j)^2)z_{m-i,n-j}(t) = \frac{1}{\epsilon}\mathcal{C}_{m,n}(t).\end{aligned} \tag{4.5}$$

In (4.5), we will use an initial condition $z_{m,n}(0,x)$. To solve (4.5) we use, for the discretization in time, a Runge-Kutta method (ode45).

4.2. **Comparison Two-Scale Numerical Solution and reference solution.** In this paragraph, we consider the truncated solution $z_P^\epsilon(t, x_1, x_2)$ and $Z_P(t, \frac{t}{\epsilon}, x_1, x_2)$. The objective here is to compare for a fixed ϵ and a given time, the quantity $|z_P^\epsilon(t, x_1, x_2) - Z_P(t, \frac{t}{\epsilon}, x_1, x_2)|$ when the water velocity $\mathcal{U}$ is given.

4.2.1. *Comparisons of $z_P^\epsilon(t, x)$ and $Z_P(t, \frac{t}{\epsilon}, x)$ with $\mathcal{U}$ given by (4.6).* For the numerical simulations, concerning z^ϵ, we take $z_0(x_1, x_2) = \cos 2\pi x_1 + \cos 4\pi x_1$ and $z_0(x_1, x_2) = Z(0, 0, x_1, x_2)$. In what concerns the water velocity field, we consider the function

$$\mathcal{U}(t, \theta, x_1, x_2) = \sin \pi x_1 \sin 2\pi\theta \, \mathbf{e}_1, \tag{4.6}$$

where $\mathbf{e}_1$ and $\mathbf{e}_2$ are respectively the first and the second vector of the canonical basis of $\mathbb{R}^2$ and x_1, x_2 are the first and the second components of x.

In Figure 1 , we can see the space distribution of the first component of the velocity $\mathcal{U}$ for a given time $t = 1$ and for various values of θ: 0.3, 0.55, and 0.7. In Figure 2, we see, for a fixed point $x = (x_1, x_2)$, how the water velocity $\widetilde{\mathcal{U}}(\theta)$

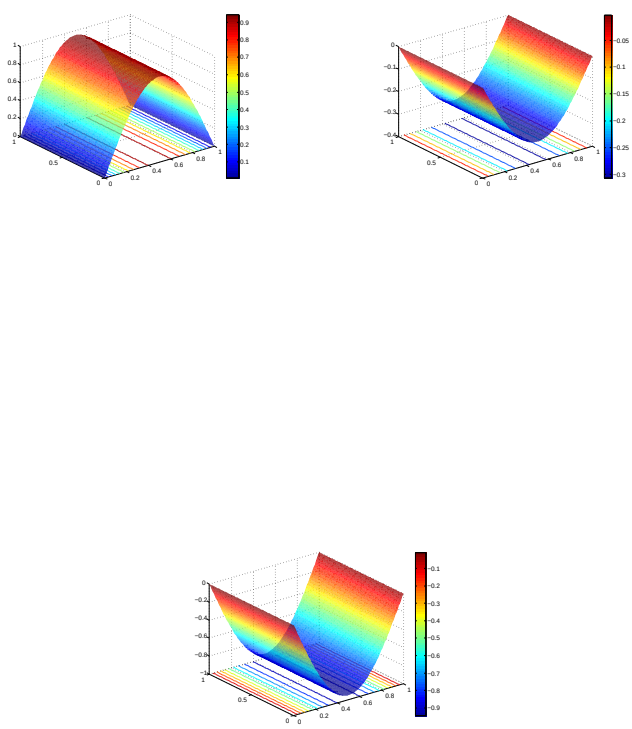

FIGURE 1. Space distribution of the first component of $\mathcal{U}(1, 0.3, (x_1, x_2))$, $\mathcal{U}(1, 0.55, (x_1, x_2))$ and $\mathcal{U}(1, 0.7, (x_1, x_2))$ when $\mathcal{U}$ is given by (4.6).

evolves with respect to θ. In Figure 3, the θ-evolution of $\widetilde{\mathcal{A}}(\theta)$ is also given in various points $(x_1, x_2) \in \mathbb{R}^2$.

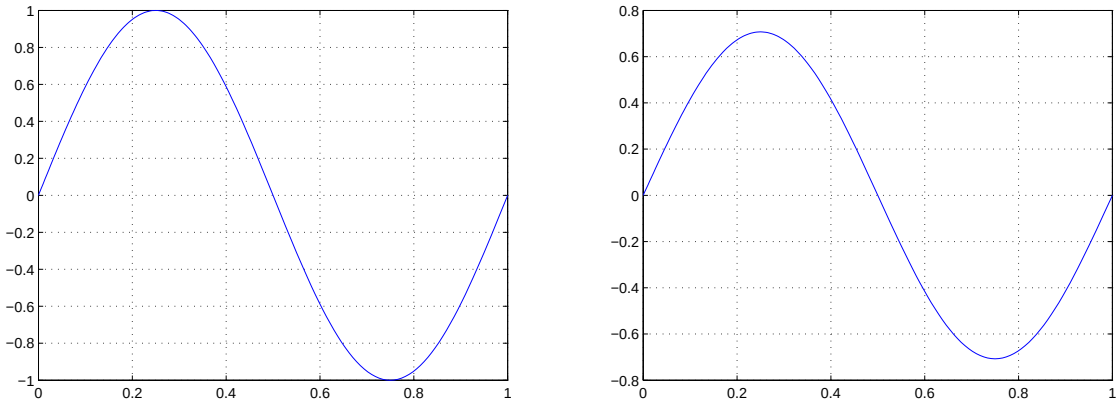

FIGURE 2. θ-evolution of $\widetilde{\mathcal{U}}(\theta,(1/2,0))$ and $\widetilde{\mathcal{U}}(\theta,(1/4,0))$ when $\mathcal{U}$ is given by (4.6)

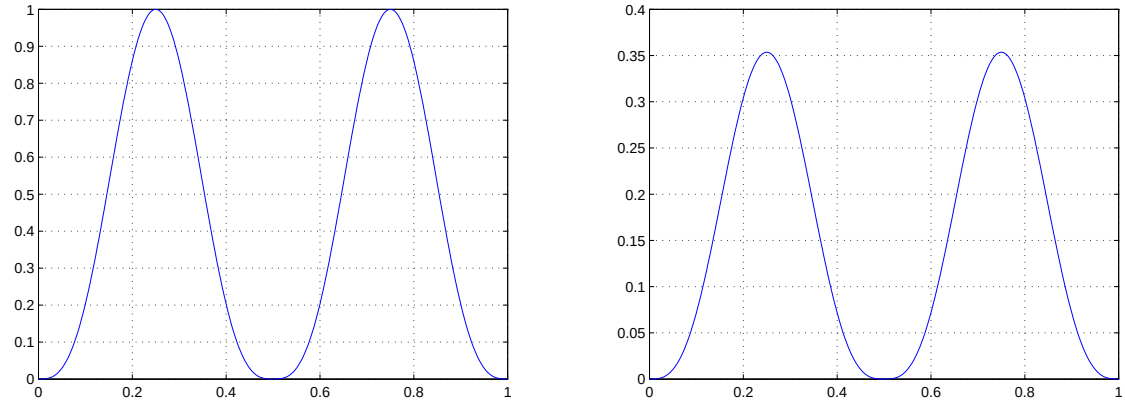

,

FIGURE 3. θ-evolution of $\widetilde{\mathcal{A}}(\theta,(1/2,0))$ and $\widetilde{\mathcal{A}}(\theta,(1/4,0))$ when $\mathcal{U}$ is given by (4.6)

In this paragraph, we present numerical simulations in order to validate the Two-Scale convergence presented in Theorem 1.1. For a given ϵ, we compare $Z_P(t,\frac{t}{\epsilon},x)$, where Z_P is the Fourier expansion of order P of the solution to (1.10) and $z_P^\epsilon(t,x)$ the Fourier expansion of order P of the solution to the reference problem. The simulations presented are given for $P=4$. The calculation of $z_P^\epsilon(t,x)$ implies knowledge of $z_0(x)$. For an initial condition $z_0(x)$ well prepared and equal to $Z(0,0,x)$, we obtain the results of Figure 4 and we remark that the results obtained are the same for $z_P^\epsilon(t,x)$ and $Z_P(t,\frac{t}{\epsilon},x)$.

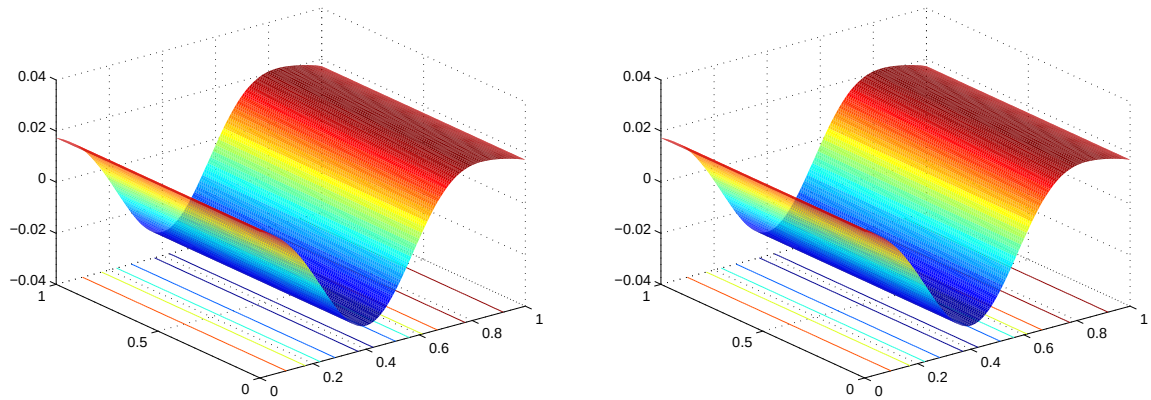

FIGURE 4. Comparison of $z^\epsilon_P(t,\cdot)$ and $Z_P(t,\frac{t}{\epsilon},\cdot)$, $P=4$, at time $t=1$, $\epsilon=0.001$, when $\mathcal{U}$ is given by (4.6) and when $z_0(\cdot)=Z(0,0,\cdot)$. On the left $z^\epsilon_P(t,\cdot)$, on the right $Z_P(t,\frac{t}{\epsilon},\cdot)$.

In practice, the solution Z_P, $P\in\mathbb{N}$ evolves according to P. For the simulations, we made the value of the integer P vary and we saw that this variation is very low from $P\geq 6$.
To better show that $Z_P(t,\frac{t}{\epsilon},x_1,x_2)$ is close to the reference solution $z^\epsilon_P(t,x_1,x_2)$, we plot and compare $Z_P(t,\frac{t}{\epsilon},x_1,0)$ and $z^\epsilon_P(t,x_1,0)$, at different times t. In these comparisons the initial condition $z_0(x_1,x_2)=\cos 2\pi x_1+\cos 4\pi x_1$ is different from $Z(0,0,x_1,x_2)$. The results are shown in Figure 5 and Figure 6. We see in these figures that the solution $z^\epsilon_P(t,x)$ get closer and closer to $Z_P(t,\frac{t}{\epsilon},x)$ with time of order ϵ.

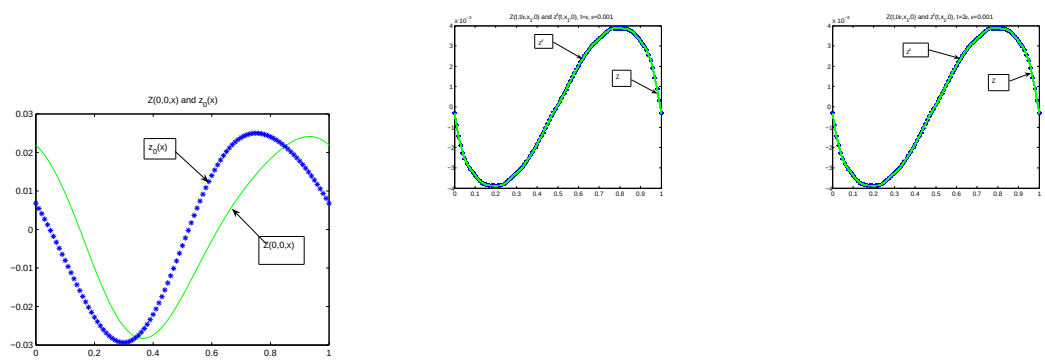

FIGURE 5. Comparison of $z^\epsilon_P(t,x_1,0)$ and $Z_P(t,\frac{t}{\epsilon},x_1,0))$, $P=4$. On the left $t=0$, in the middle $t=\epsilon$ and $t=2\epsilon$ on the right, $\epsilon=0.001$.

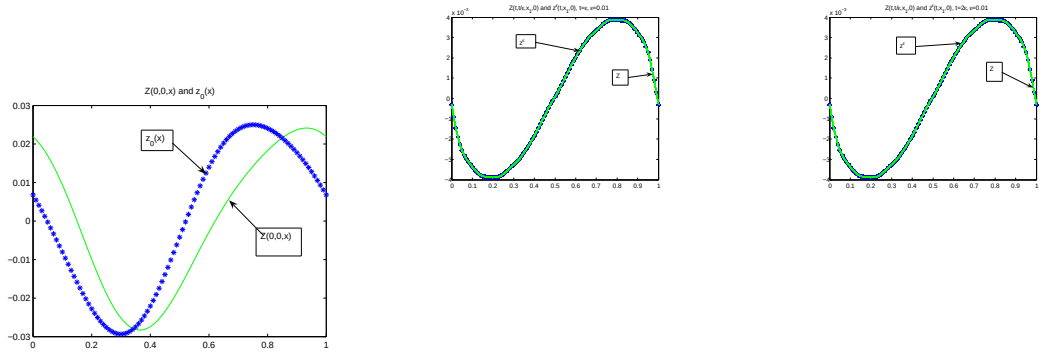

FIGURE 6. Comparison of $z_P^\epsilon(t, x_1, 0)$ and $Z_P(t, \frac{t}{\epsilon}, x_1, 0))$. On the left $t = 0$, in the middle $t = \epsilon$ and $t = 2\epsilon$ on the right, $\epsilon = 0.01$.

So we can see from these figures that the solution Z of the Two-Scale limit problem is such that $Z(t, \frac{t}{\epsilon}, \cdot, \cdot)$ is close to the solution $z^\epsilon(t, \cdot, \cdot)$ of the reference problem. In the presently considered case where the initial condition for z^ϵ is not $Z(0, 0, \cdot, \cdot)$, we saw in Figure 5 and Figure 6 that z_P^ϵ tends to reach a steady state. This steady state is an oscillatory one in the sense that for large t, $z_P^\epsilon(t, \cdot, \cdot)$ behaves like $Z_P(t, \frac{t}{\epsilon}, \cdot, \cdot)$. This is illustrated by Figure 7 where $z_P^\epsilon(t, x_1, 0)$ and $Z_P(t, \frac{t}{\epsilon}, x_1, 0)$ are given for various value of t in a period of lenght ϵ.
More precisely, in this figure we see that within a period of time of lenght ϵ, $z_P^\epsilon(t, \cdot, \cdot)$ and $Z_P(t, \frac{t}{\epsilon}, \cdot, \cdot)$ do not glue together completly. Nevertheless, despite this phenomenon which is linked with the fact that the Two-Scale approximation of $z^\epsilon(t, \cdot, \cdot)$ by $Z(t, \frac{t}{\epsilon}, \cdot, \cdot)$ is only of order 1 in ϵ, the two solutions re-glue well together at the end of the period.

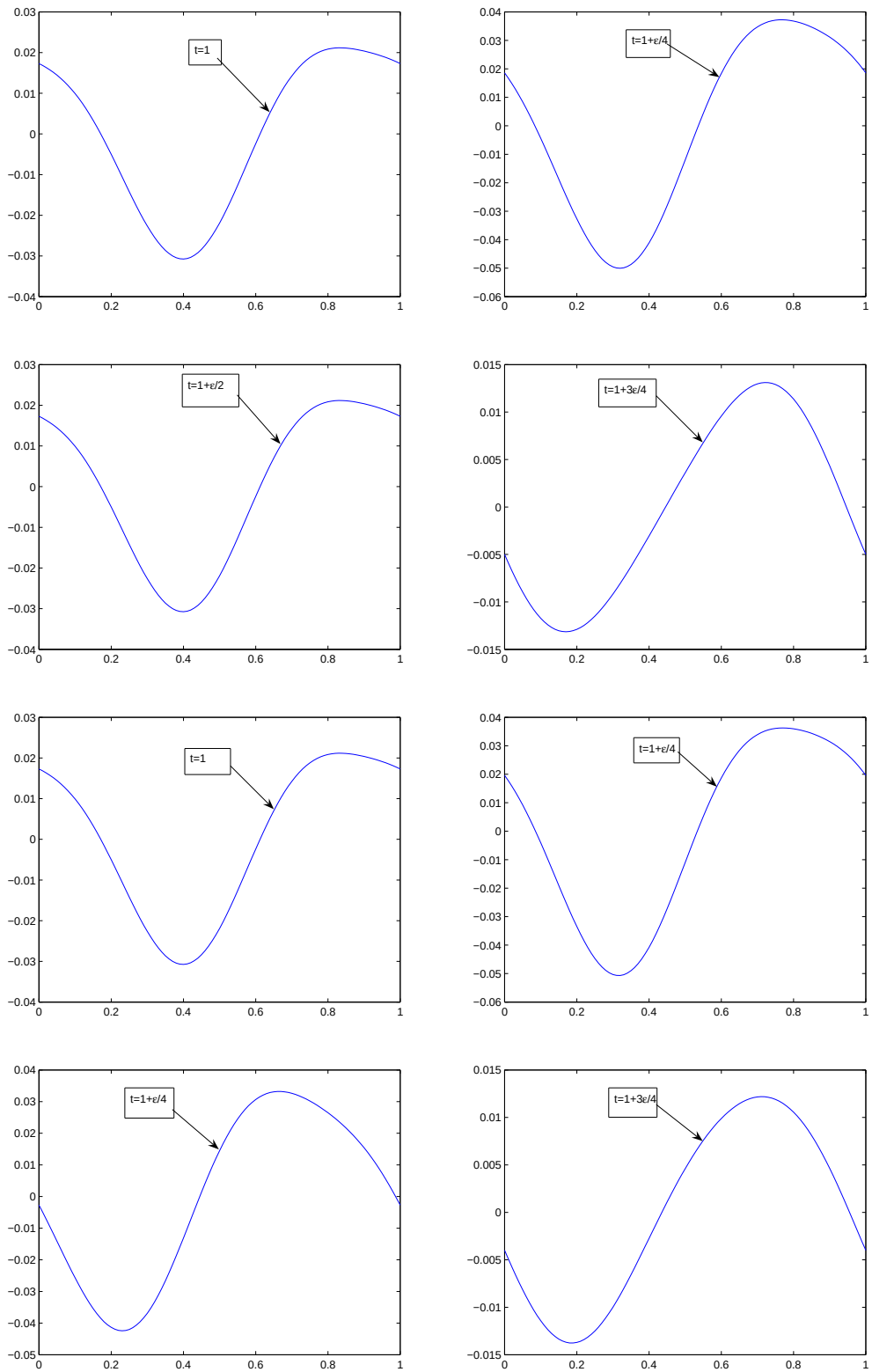

FIGURE 7. Evolution of $Z_P(t, \frac{t}{\epsilon}, x_1, 0)$ in the top and $z_P^\epsilon(t, x_1, 0)$ in the bottom, $t = 1 + \frac{n\epsilon}{4}$, $n = 0, 1, 2, 3$.

4.2.2. *Comparisons of $z^\epsilon(t,x)$ and $Z(t,\frac{t}{\epsilon},x)$ with $\mathcal{U}$ is given by (4.7).* In this subsection, we do the same as in the precedent one, but when the velocity fields $\mathcal{U}$ given by (4.7). The results are all identical to the precedent one i.e. the Two-Scale limit $Z_P(t,\frac{t}{\epsilon},x_1,x_2)$ is very close to the solution $z_P^\epsilon(t,x_1,x_2)$ to the reference problem when $P=4$. The initial condition $z_0(x_1,x_2)\neq Z(0,0,x_1,x_2)$ and is the same as in the subsection 4.2.1. The results are given for $\epsilon=0.1$ and $\epsilon=0.005$ and for various time t. We notice that z^ϵ comes very close to $Z(t,\frac{t}{\epsilon},x_1,x_2)$ when ϵ is very small. We begin by giving the space distribution of $\mathcal{U}$ at various time and the $\theta-$evolution of $\mathcal{U}$ and $\widetilde{\mathcal{A}}$. The second velocity fields is given by

$$\mathcal{U}(t,\theta,x_1,x_2)=\mathcal{U}(t,\theta,x)=\begin{cases} 0 \text{ in } [0,\theta_1],\\ \frac{\theta-\theta_1}{\theta_2-\theta_1}U_{thr}\mathbf{e}_2 \text{ in } [\theta_1,\theta_2],\\ U_{thr}\mathbf{e}_2+\phi(\frac{\theta-\theta_2}{\theta_3-\theta_2})\psi(t,x) \text{ in } [\theta_2,\theta_3],\\ \frac{\theta-\theta_3}{\theta_4-\theta_3}U_{thr}\mathbf{e}_2 \text{ in } [\theta_3,\theta_4],\\ 0 \text{ in } [\theta_4,\theta_5],\\ \frac{\theta-\theta_5}{\theta_6-\theta_5}U_{thr}\mathbf{e}_2 \text{ in } [\theta_5,\theta_6],\\ -U_{thr}\mathbf{e}_2-\phi(\frac{\theta-\theta_6}{\theta_7-\theta_6})\psi(t,x) \text{ in } [\theta_6,\theta_7],\\ -\frac{\theta-\theta_7}{\theta_8-\theta_7}U_{thr}\mathbf{e}_2 \text{ in } [\theta_7,\theta_8],\\ 0 \text{ in } [\theta_8,1], \end{cases} \tag{4.7}$$

where $U_{thr}>0$, ϕ is a regular positive function satisfying $\phi(s)=s(1-s)$ and $\psi(t,x_1)=(1+\sin\frac{\pi}{30}t)(U_{thr}\mathbf{e}_2+\frac{1}{10}(1+\sin 2\pi x_1)\mathbf{e}_1)$, $\theta_i=\frac{i+1}{10}$, $i=1,\dots,8$.
The θ-evolution of $\mathcal{U}$, given by (4.7), is given in Figure 9 for various position in $[0,1]^2$.
Function $g_a(\mathbf{u})=g_c(\mathbf{u})=|\mathbf{u}|^3, a=c=1$ and $\mathcal{M}(t,\theta,x)=0$ which yields a θ-evolution of $\widetilde{\mathcal{A}}(\theta)$ which is drawn for various positions in Figure 10.

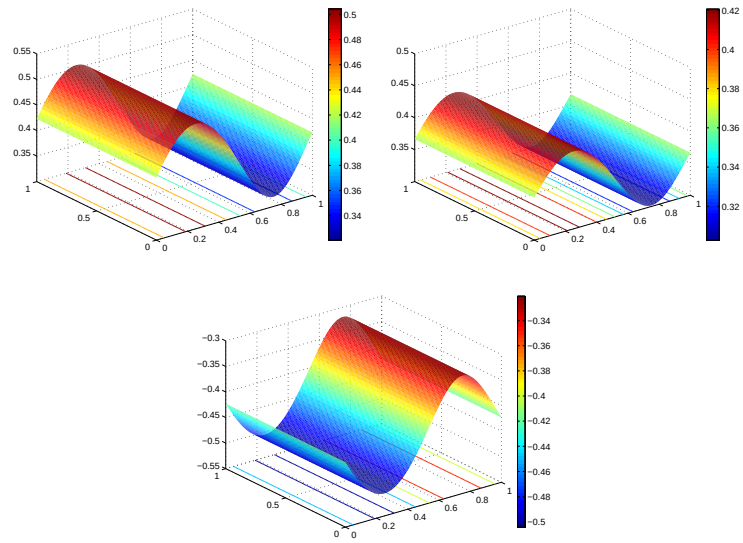

FIGURE 8. Space distribution of the first component of $\mathcal{U}(1, 0.25, (x_1, x_2))$, $\mathcal{U}(1, 0.275, (x_1, x_2))$ and $\mathcal{U}(1, 0.75, (x_1, x_2))$ when $\mathcal{U}$ is given by (4.7).

Using this, we compute $Z_P(t, \frac{t}{\epsilon}, x_1, x_2)$ and $z^\epsilon_P(t, x)$ for $P = 4$. To compute $z^\epsilon_P(t, x)$ we take $z_0(x_1, x_2) = \cos 2\pi x_1 + \cos 4\pi x_1$ which is not $Z(0, 0, x_1, x_2)$. First we study the errors $Z_P(t, \frac{t}{\epsilon}, x_1, x_2) - z^\epsilon_P(t, x)$ at $t = 1$. This quantity decreases when ϵ decreases as illustrated in the following tabular.

value of ϵ	norm L^1	norm L^2	norm L^∞
0.01	0.012212	0.00048013	0.003376
0.03	0.019082	0.0005753	0.0017347
0.05	0.030769	0.01348	0.0069818
0.07	0.045123	0.029055	0.009
0.09	0.17067	0.10562	0.038790
0.1	0.3053	0.10562	0.04878

Table: Errors norm $Z_P(t, \frac{t}{\epsilon}, x_1, x_2) - z^\epsilon_{\tilde{P}}(t, x_1, x_2)$, $\tilde{P} = (4, 4)$, $P = (4, 4, 4)$, $t = 1$.

The results given in this table show that, at time $t = 1$, $z^\epsilon(t, x)$ is closer to $Z(t, \frac{t}{\epsilon}, x)$ when ϵ is very small. These results validate the results obtained in Theorem 1.1.

In Figures 11 and 12, we present simulations at times $t = 0.75$ and $t = 0.775$. We see that $Z_P(t, \frac{t}{\epsilon}, x_1, x_2)$ is close to $z^\epsilon_P(t, x_1, x_2)$. The numerical results shown in these figures are made with $\epsilon = 0.1$.

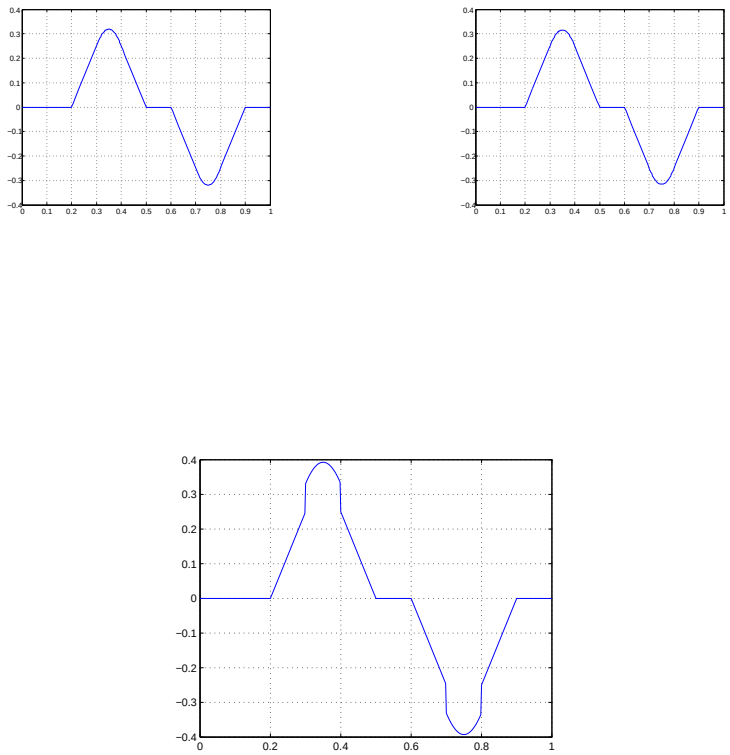

FIGURE 9. θ-evolution of $\mathcal{U}(1,\theta,(1,0))$, $\mathcal{U}(1,\theta,(4,0))$ and $\mathcal{U}(1,\theta,(1/3,1/3))$ when $\mathcal{U}$ is given by (4.7).

In Figure 13 and 14, we do the same but for $\epsilon = 0.005$. The numerical results show that $z_P^\epsilon(t,x)$ is also very close to $Z_P(t,\frac{t}{\epsilon},x_1,x_2)$.

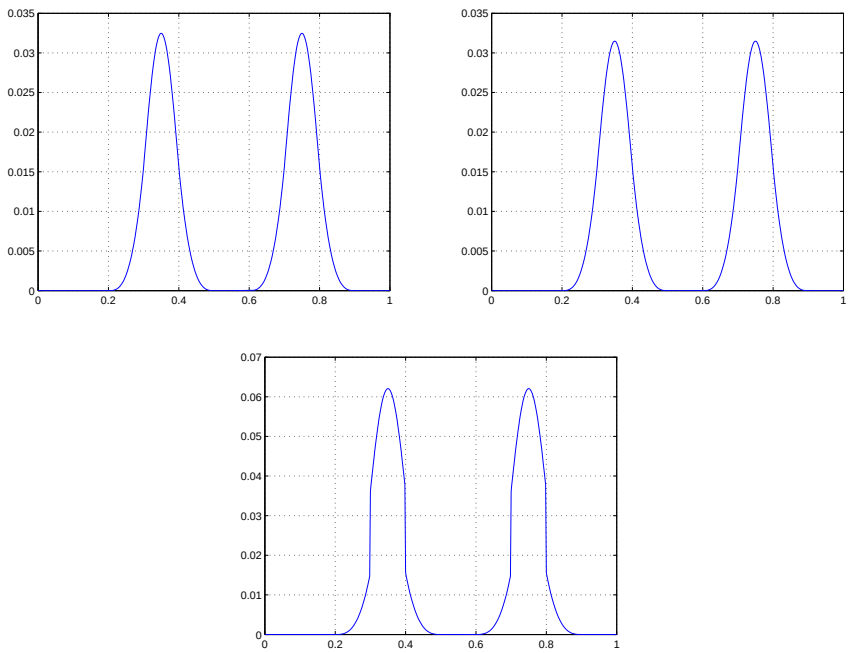

FIGURE 10. θ-evolution of $\widetilde{\mathcal{A}}(1,\theta,(1,0))$, $\widetilde{\mathcal{A}}(1,\theta,(4,0))$ and $\widetilde{\mathcal{A}}(1,\theta,(1/3,1/3))$ when $\mathcal{U}$ is given by (4.7).

We remark that for $\epsilon = 0.1$ and $\epsilon = 0.005$, the solution $z_P^\epsilon(t,x)$ is very close to $Z_P(t,\frac{t}{\epsilon},x)$. But the approximation $z_P^\epsilon(t,x) \sim Z_P(t,\frac{t}{\epsilon},x)$ is very good when ϵ is very small.
To show that z_P^ϵ is very close to Z_P, we construct the same figures as previously but in dimension 2 with $\epsilon = 0.005$ i.e. we construct $z_P^\epsilon(t,x_1,0)$ and $Z_P(t,\frac{t}{\epsilon},x_1,0)$ for $\epsilon = 0.005$ at time $t = 0.775$. This is given in Figure 15.

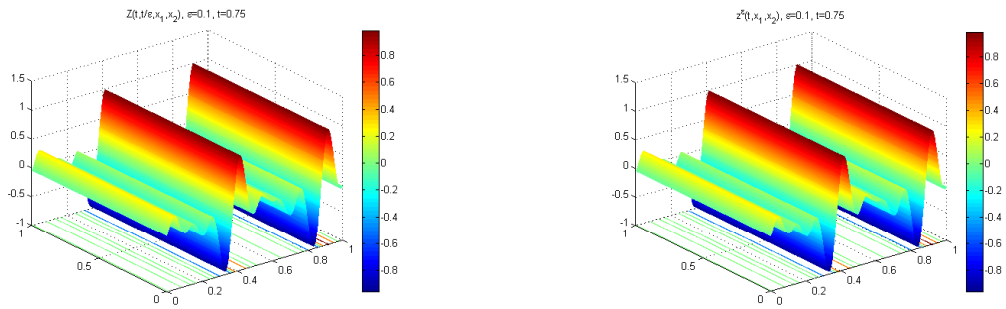

FIGURE 11. Comparison of $z_P^\epsilon(t, x_1, x_2)$ and $Z_P(t, \frac{t}{\epsilon}, x_1, x_2)$, $P = 4$; $t = 0.75$, $\epsilon = 0.1$, $z_0(x_1, x_2) = \cos 2\pi x_1 + \cos 4\pi x_1$. On the left $Z_P(t, \frac{t}{\epsilon}, x_1, x_2)$, on the right $z_P^\epsilon(t, x_1, x_2)$.

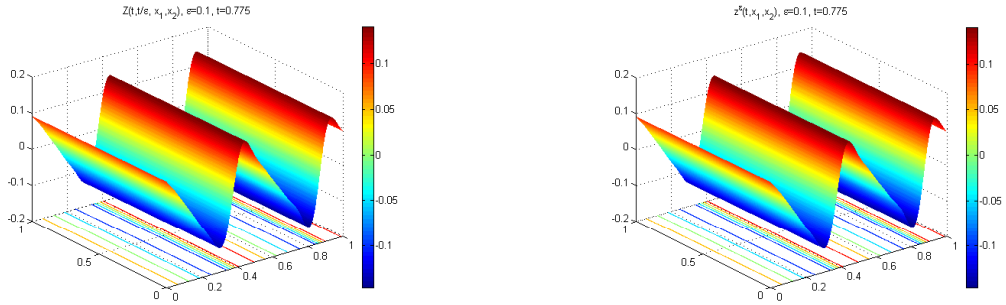

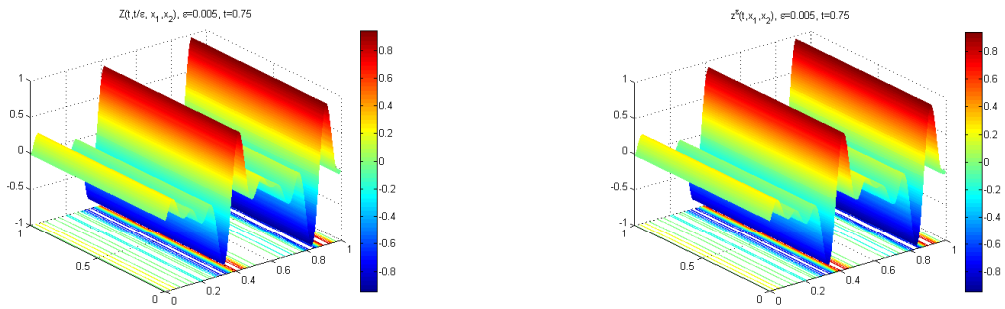

FIGURE 13. Comparison of $z_P^\epsilon(t, x_1, x_2)$ and $Z_P(t, \frac{t}{\epsilon}, x_1, x_2)$, $P = 4$; $t = 0.75$, $\epsilon = 0.005$, $z_0(x_1, x_2) = \cos 2\pi x_1 + \cos 4\pi x_1$. On the left $Z_P(t, \frac{t}{\epsilon}, x_1, x_2)$, on the right $z_P^\epsilon(t, x_1, x_2)$.

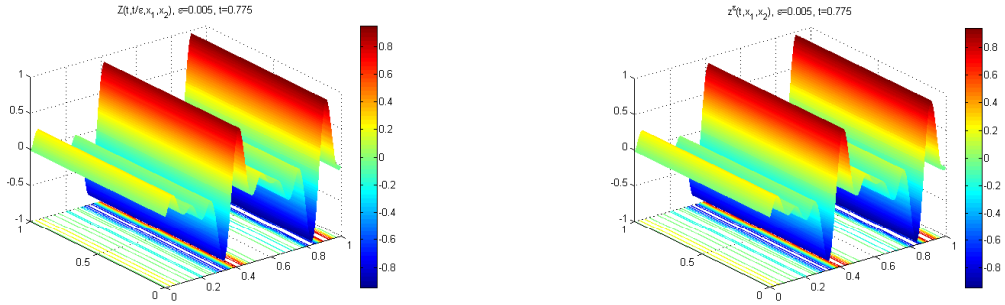

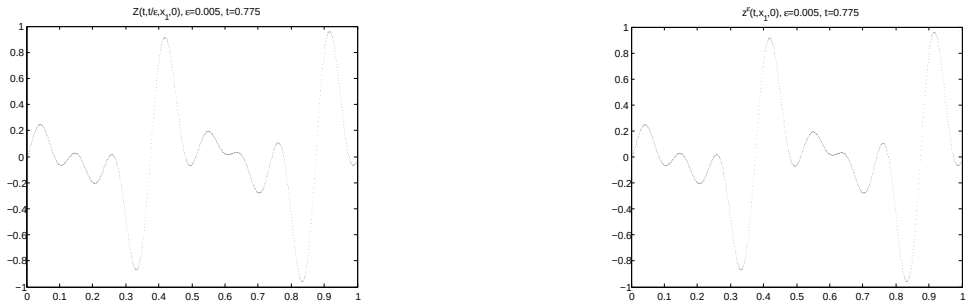

FIGURE 15. Comparison of $z_P^\epsilon(t, x_1, 0)$ and $Z_P(t, \frac{t}{\epsilon}, x_1, 0)$, $t = 0.775$, $\epsilon = 0.005$. On the left $Z_P(t, \frac{t}{\epsilon}, x_1, 0)$, on the right $z_P^\epsilon(t, x_1, 0)$.

The results in Figure 16 show that Z_P and z_P^ϵ have the same behavior in the same period and Z_P is very close to z_P^ϵ. We also notice that, despite the small shifts that occur during a period, the two solutions glue together.

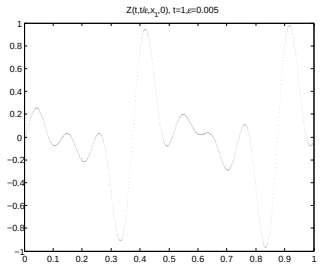
Z(t,t/ε,x_1,0), t=1,ε=0.005

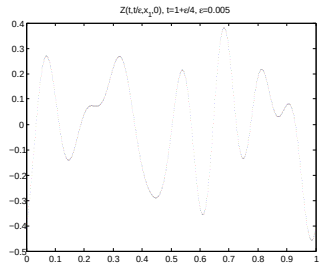
Z(t,t/ε,x_1,0), t=1+ε/4, ε=0.005

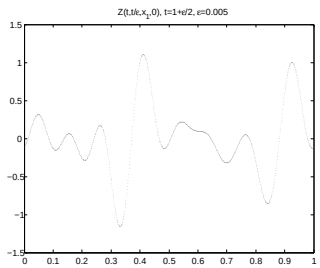
Z(t,t/ε,x_1,0), t=1+ε/2, ε=0.005

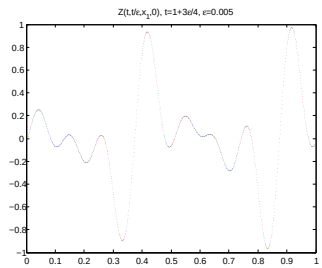
Z(t,t/ε,x_1,0), t=1+3ε/4, ε=0.005

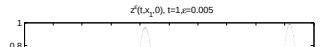
z^0(t,x_1,0), t=1,ε=0.005

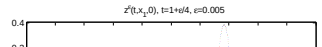
z^0(t,x_1,0), t=1+ε/4, ε=0.005

REFERENCES

[1] G. Allaire, *Homogenization and Two-Scale convergence*, SIAM J. Math. Anal. **23** (1992), 1482–1518.

[2] P. Aillot, E. Frénod, V. Monbet, *Long term object drift in the ocean with tide and wind*. Multiscale Modelling and Simulation, 5, 2(2006), 514-531.

[3] I. Faye, E. Frénod, D. Seck, *Singularly perturbed degenerated parabolic equations and application to seabed morphodynamics in tided environment*,Discrete and Continuous Dynamical Systems, Vol 29 N^o3 March 2011, pp 1001-1030.

[4] E. Frénod , A. Mouton, *Two-dimensional Finite Larmor Radius approximation in canonical gyrokinetic coordinates*. Journal of Pure and Applied Mathematics: Advances and Applications, Vol 4, No 2 (2010), pp 135-166.

[5] E. Frénod, A. Mouton, E. Sonnendrücker *Two-Scale numerical simulation of the weakly compressible 1D isentropic Euler equations*. Numerishe Mathematik,(2007) Vol 108, No2, pp 263293 (DOI : 10.1007/s00211-007-0116-8).

[6] E. Frénod, F. Salvarani, E. Sonnendrücker, *Long time simulation of a beam in a periodic focusing channel via a Two-Scale PIC-method*. Mathematical Models and Methods in Applied Sciences, Vol. 19, No 2 (2009) pp 175–197 (DOI No: 10.1142/S0218202509003395).

[7] E. Frénod, Raviart P. A., and E. Sonnendrücker, *Asymptotic expansion of the Vlasov equation in a large external magnetic field*, J. Math. Pures et Appl. **80** (2001), 815–843.

[8] O. A. Ladyzenskaja, V. A. Solonnikov, and N. N. Ural'ceva, "Linear and quasi-linear equations of parabolic type", AMS Translation of Mathematical Monographs **23** (1968).

[9] A. Mouton, *Approximation multi-échelles de l'équation de Vlasov*, thèse de doctorat, Strasbourg 2009.

[10] A. Mouton, *Two-Scale semi-Lagrangian simulation of a charged particules beam in a periodic focusing channel*, Kinet. Relat. Models, **2**-2(2009), 251-274.

[11] G. Nguetseng, *A general convergence result for a functional related to the theory of homogenization*, SIAM J. Math. Anal. **20** (1989), 608–623.

E-mail address: `ibrahima.faye@uadb.edu.sn`
E-mail address: `emmanuel.frenod@univ-ubs.fr`
E-mail address: `diaraf.seck@ucad.edu.sn`